Aerospace Structures Information and Analysis Center

Non-Linear Finite Element Analysis of Viscoelastic Materials

Report No. TR-98-02

July 1998

Approved for Public Release; Distribution is Unlimited

Operated for the Flight Dynamics Directorate by CSA Engineering, Inc.

FOREWORD

This report was prepared by the Aerospace Structures Information and Analysis Center (ASIAC), which is operated by CSA Engineering, Inc. under contract number F33615-94-C-3200 for the Air Vehicles Directorate, Wright-Patterson Air Force Base, Ohio. The report presents the work performed under ASIAC Task No. T-41. The work was sponsored by the Vibration and Aeroelasticity Branch, Structures Division, Air Vehicles Directorate of the Air Force Research Laboratory at WPAFB, Ohio. The technical monitor for the task was Mr. Robert Gordon of the Vibration and Aeroelasticity Branch. The study was performed by Mr. Gordon Negaard, CSA Engineering Inc.

This technical report covers work accomplished from September, 1997 through July 1998.

TABLE OF CONTENTS

LIST OF FIGURES

1.0 INTRODUCTION

Many aircraft structures and engine components are subjected to extreme aero-vibroacoustic environments, including high g-loads. High cycle fatigue due to resonant vibrations on these components causes cracking and other degradation that reduces both operational capability and life. It would be useful if viscoelastic materials could be used to damp the vibration of such structures, however the behavior of a viscoelastic material in an extremely high g-loading is not well understood. The objective of this study was to investigate the need to account for the non-linear material characteristics of viscoelastic materials in order to obtain accurate stress distribution predictions. This will contribute to understanding the appropriate analytical procedure(s) for use in designing viscoelastic damping material into gas-turbine blades.

Because of the limited resources allotted to the task, an existing finite element model was used and the results from ABAQUS, a finite element code with nonlinear analysis capabilities, are compared to previous linear elastic results obtained with NASTRAN in a previous study. This model represented a rotor blade spinning at 7,500 rpm which results in a g-load of approximately 25,000 at the tip of a fifteen inch radius blade. The finite element model represented an eight inch wide blade with a viscoelastic filled cavity or pocket near the tip. This cavity extended from 13.875 inches to 14.875 inches in the radial direction , which left a one-eighth inch containing wall at the tip. The cavity thickness was 0.06 inches with similar cavity wall thicknesses giving a total blade thickness of 0.18 inches at the blade tip. A fabrication drawing of this ``pocket'' part of the blade is shown in Figure 1 below.

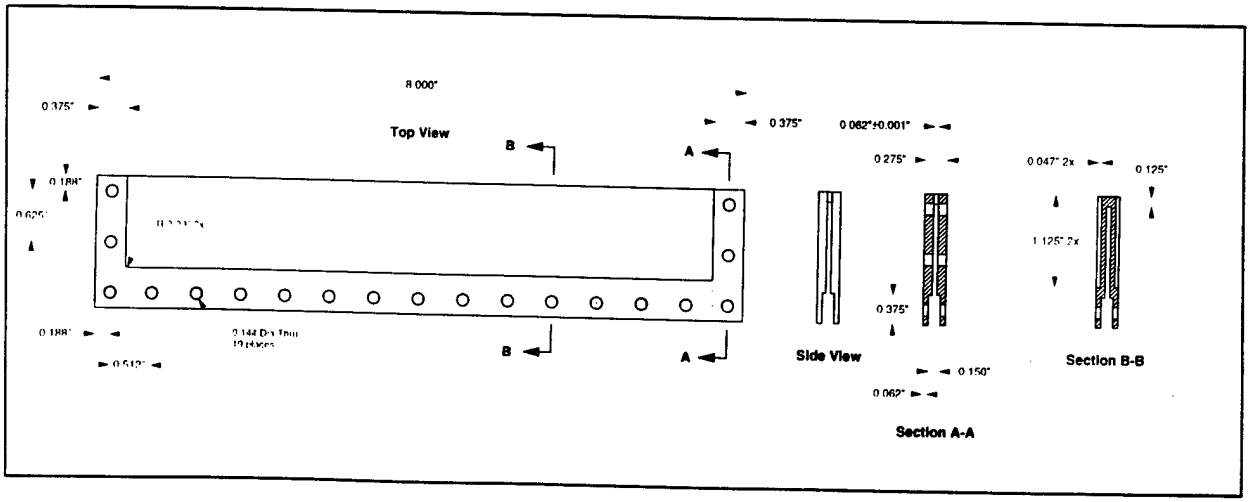

Figure 1. Drawing illustrating the viscoelastic cavity dimensions.

2.0 TECHNICAL APPROACH

A primary concern leading to the request for this study is that hydrostatic-type loading in the cavity due to body forces under a high-g rotational field may cause internal pressures that will rupture or deform the cavity walls. It has also been assumed that viscoelastic material (VEM) may act like a rubbery material and be almost incompressible, with the Poisson's ratio, υ, approaching a value of one-half. This is difficult to study with a linear elastic finite element code like NASTRAN since the code becomes algorithmically unstable as υ approaches one-half. In a previous linear elastic study (Ref 1), cavity pressure and shear stresses were obtained for υ as high as 0.499999 with credible accuracy and behavior but at this point the analysis failed to converge.

For the linear elastic analyses, a shear modulus, G, of 200 and 1,200 psi was assumed and υ was varied from 0.40 to 0.499999. Regardless of the values used, the behavior of the VEM was qualitatively the same. A certain amount of hydrostatic pressure was observed near the bottom of the cavity, but the shear on the walls appeared to prevent significant hydrostatic pressure from building up in the remainder of the cavity. It was found that the shear angle, τ_{rz}, in the viscoelastic medium was large (as much as twenty degrees) at the top of the cavity. A plot of this behavior is depicted in Figure 2. The outer radius of the VEM is referred to as the base or bottom of the cavity and the innermost radius of the VEM is the top of the cavity. In the following plots, the pressures and shear stresses are then measured from zero at the base of the cavity to one inch at the top of cavity

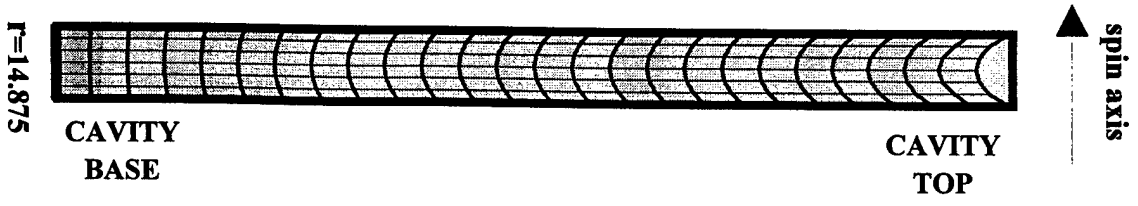

Figure 2. Plot illustrating the deformation of the viscoelastic material under a rotational force.

Nonlinear analysis steps define a sequence of events that follow one another, in the sense that the state of the model at the end of a step provides the initial conditions for the start of the next step. This is useful for large displacement problems and necessary if the material is nonlinear with load history. Both NASTRAN and ABAQUS have a piecewise continuous capability which provides solutions for a series of increments on the load-displacement path. Because the large shears meant that relatively large displacements and deformations were taking place in the finite elements at the top of the cavity, a piecewise linear analysis was run on both NASTRAN and ABAQUS to see if geometric nonlinearity was occurring. The results were identical to the linear analyses, indicating that, in this model at least, the large shear displacements were not a problem. The question remains as to whether a linear elastic analysis adequately models the behavior of the material itself under a high-g load and whether a material non-linearity exists and that creep under a high centrifugal force may increase the hydrostatic pressure significantly.

To study the incompressibility assumption, the hyperelastic option in ABAQUS was used. The hyperelastic element in ABAQUS is designed to describe the behavior of materials that exhibit elastic response up to large strains, as rubber, solid propellant, and other elastomeric materials. Most solid rubber like materials are almost incompressible and have a bulk modulus, K, that is several orders of magnitude larger than their shear modulus, G. These materials are described in terms of a ``strain energy potential'', U, which defines the strain energy stored in the material per unit volume in the initial configuration as a function of the strain at that point in the material. The hyperelastic option only allows the user to input values for G and K. Therefore G was again kept constant at 200 psi while K was varied from 50,000 to 1,000,000, roughly two to four orders of magnitude larger than G. These nonlinear results were then compared to the linear elastic results from ABAQUS.

Finally, to complete the study, a theoretical analysis was done to determine if there were limits on shear modulus and cavity thickness that could be used as safety factors in designing damping cavities within blades. Another question attempted was whether a shift in center of gravity of the blade due to compressive displacement of the VEM could be a factor to consider.

3.0 RESULTS OF LINEAR ELASTIC ANALYSIS

The finite element model used for this study was created using 8-noded solid elements to represent both the VEM filled cavity and the walls surrounding the pocket. In order to obtain reasonable stress distributions in the thickness and radial directions of the blade, each element was defined as 0.01 inch in the thickness or "z" direction and 0.04 inches in the radial direction. This allowed six elements through the thickness of the cavity as well as six elements through each wall thickness. The existing NASTRAN model was converted to an ABAQUS model using PATRAN. Boundary and loading conditions had to be inserted by hand because of differences in the two programs. Running both models as solid metal blades produced identical deformations and stresses, indicating the two models were exactly identical in behavior. Linear elastic analyses were then run on both NASTRAN and ABAQUS to obtain deformation, pressure stresses, and shear stresses in the VEM. The hydrostatic pressures in the VEM are plotted in figure 3 below.

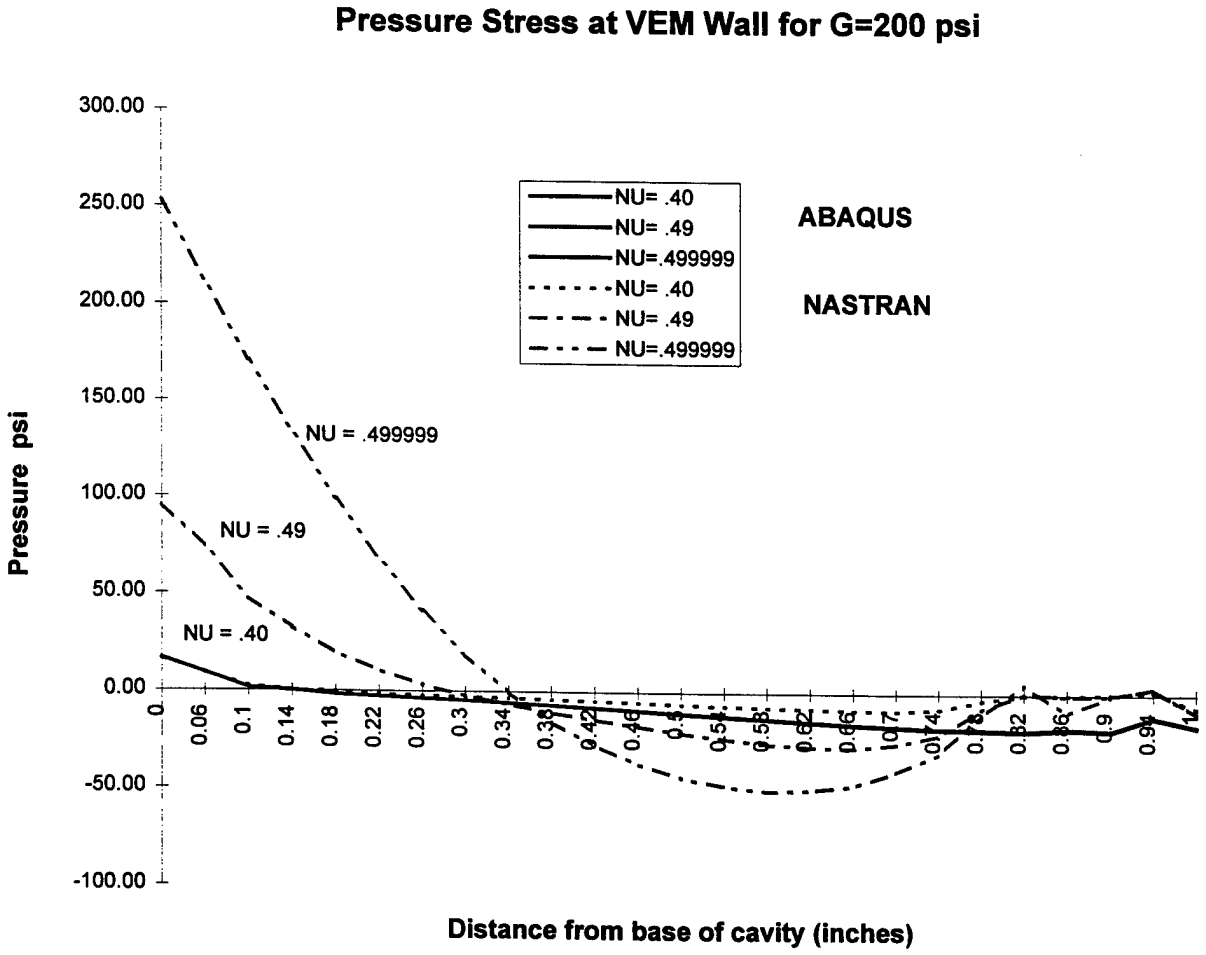

Figure 3. Plot illustrating the hydrostatic pressure stresses in the VEM from linear elastic analyses .

The results show that variations in Poisson's ratio had only a minute effect on the hydrostatic pressures calculated by ABAQUS, whereas NASTRAN predicted higher and higher pressures at the base of cavity as υ approached 0.5, approaching incompressibility. For all cases, the pressure drops rapidly and becomes negative in the upper part of the cavity, putting the VEM is in tension rather than compression. A second difference in the analysis is that ABAQUS predicts tension the rest of the way to the top surface, whereas NASTRAN results show the pressure returning to zero at the free surface.

The question is which behavior is physically correct? Qualitatively, it seems clear that the hydrostatic pressure is the highest at the base of the cavity and that the compression of this material and possible bulging of the container walls is countered by a shear stress along the cavity walls which resists centrifugal displacement of the VEM. The behavior of this shear stress is depicted in figure 4.

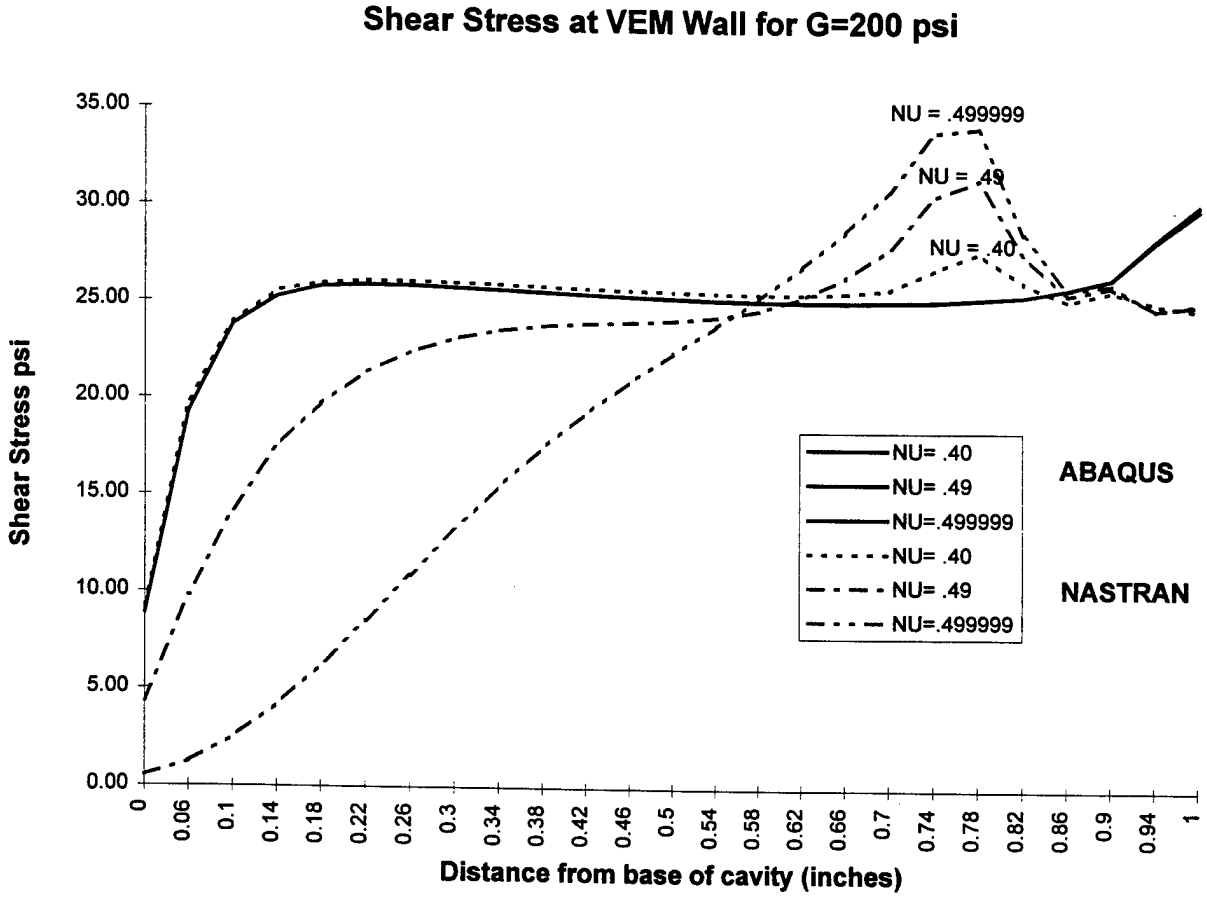

Figure 4. Plot illustrating the shear stresses in the VEM at the wall from linear elastic analyses .

Again, variations in Poisson's ratio had very little effect on the shear stresses calculated by ABAQUS, whereas NASTRAN shear stresses varied dramatically. The more compressible the material, the quicker the wall shear stresses rose to a maximum and where it then maintained this shear value the remainder of the way to the top surface. This behavior indicates that the VEM in the base of the cavity does behave in a hydrostatic manner at the base of the cavity, but as the material deforms, the shear at the wall increases until it is able to exert sufficient force to maintain an equilibrium with the centrifugal force. From that point, the shear should be constant, regardless of the depth of the cavity. The shear modulus, G, was varied from 200 psi to 1,200 psi to examine the effect of shear modulus. The results showed that as G increases, the shear stress rises to the equilibrium value quicker, reducing the area of hydrostatic pressure, but this equilibrium value depended only on the centrifugal force.

The strange behavior in NASTRAN stresses near the top of the cavity is caused by the boundary constraints which represent where the "pocket" is bolted to the blade. Analysis of the displacements in the cavity walls show a bulging at the base and a corresponding inward displacement in the upper half of the cavity. This can be attributed to the action of the positive and negative pressures in the VEM cavity. This creates bending in the wall surrounding the cavity and also creates bending in the viscoelastic material solidly adhering to the wall. This bending affects the shear stresses at the wall, but only to a small degree since bending is very gradual. However additional bending in the walls near the top of the cavity occurs since these bolted connections are assumed to be rigidly clamped to a metal blade, resisting rotation of the pocket wall at these points. This bending attempts to straighten the wall by bending it back to it's undeformed position. The effect is to add an additional shear angle to the shear caused by centrifugal force, causing what looks like an overshoot of the shear stress value. The "overshoot" is also seen to be a function of the incompressibility of the VEM. In any case, the conclusion is that the shear stress overshoots, particularly, should be ignored, and that the actual shear stresses at the cavity top can be assumed to be approximately the same values as depicted by the ABAQUS results.

4.0 RESULTS OF HYPERELASTIC ANALYSIS

The only change necessary to use the hyperelastic capability in ABAQUS is to change the material property cards.. There are several options available, including inputting experimentally derived data. The polynomial option was chosen because of it's simplicity. The user inputs the shear and bulk modulus directly and the material can be allowed to become fully incompressible. Figure 5 shows the hydrostatic stress in the cavity for G equals 200 psi and compares these results to the ABAQUS linear analysis. The K values were chosen because a typical VEM is assumed to have a bulk modulus of about 500,000 psi and the upper and lower limits were assumed. If we compare these results to the NASTRAN hydrostatic stresses in figure 3, we see a very similar pattern and magnitude of stress. Correcting for the difference in Poisson's ratio of the two plots, the hyperelastic analysis shows slightly higher values of hydrostatic pressure.

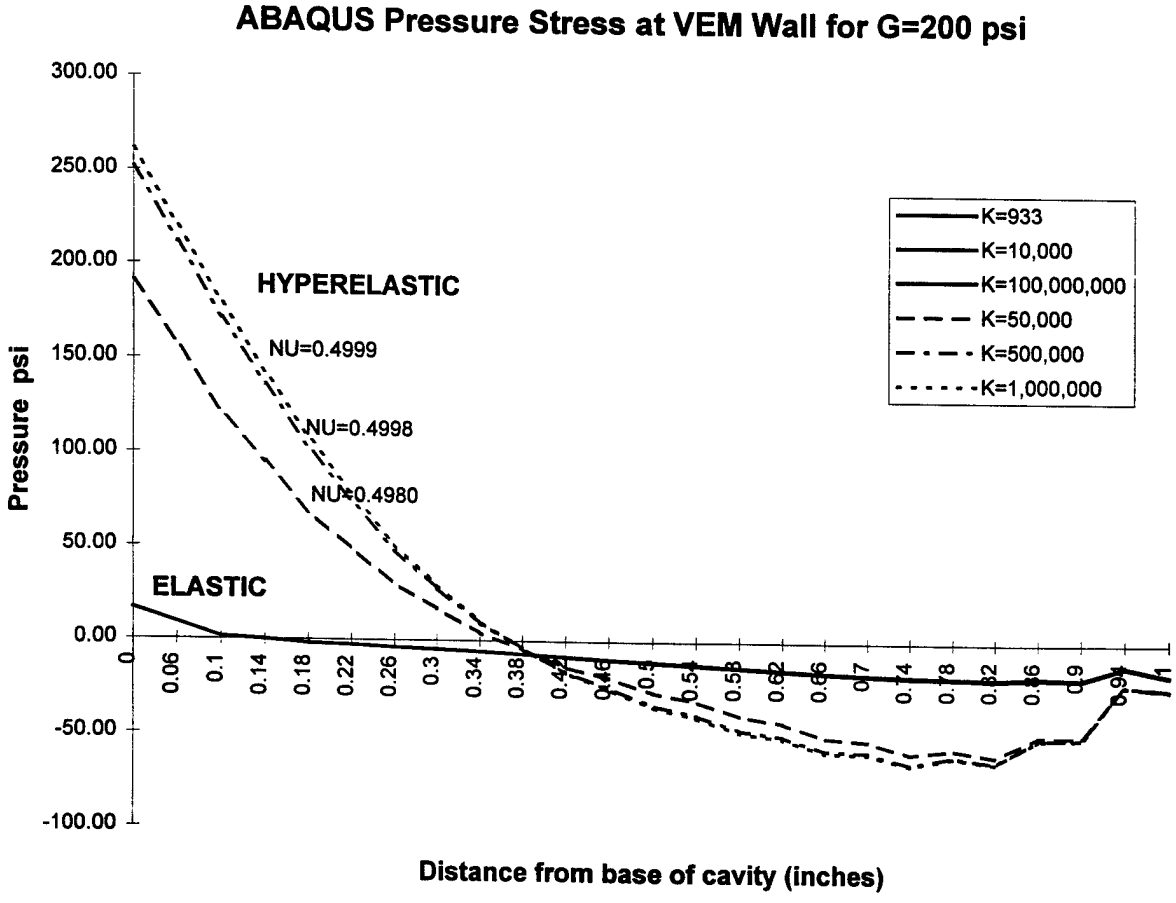

Figure 5. Plot illustrating the hydrostatic pressure stresses in the VEM from hyperelastic analyses .

As seen in Figure 6, the results from the ABAQUS shear stress also show a behavior similar to the NASTRAN results, but without the type of overshoot stresses exhibited in NASTRAN. The behavior in the lower half of the cavity is quite similar, but the behavior near the top of the cavity is much better behaved than the NASTRAN results.

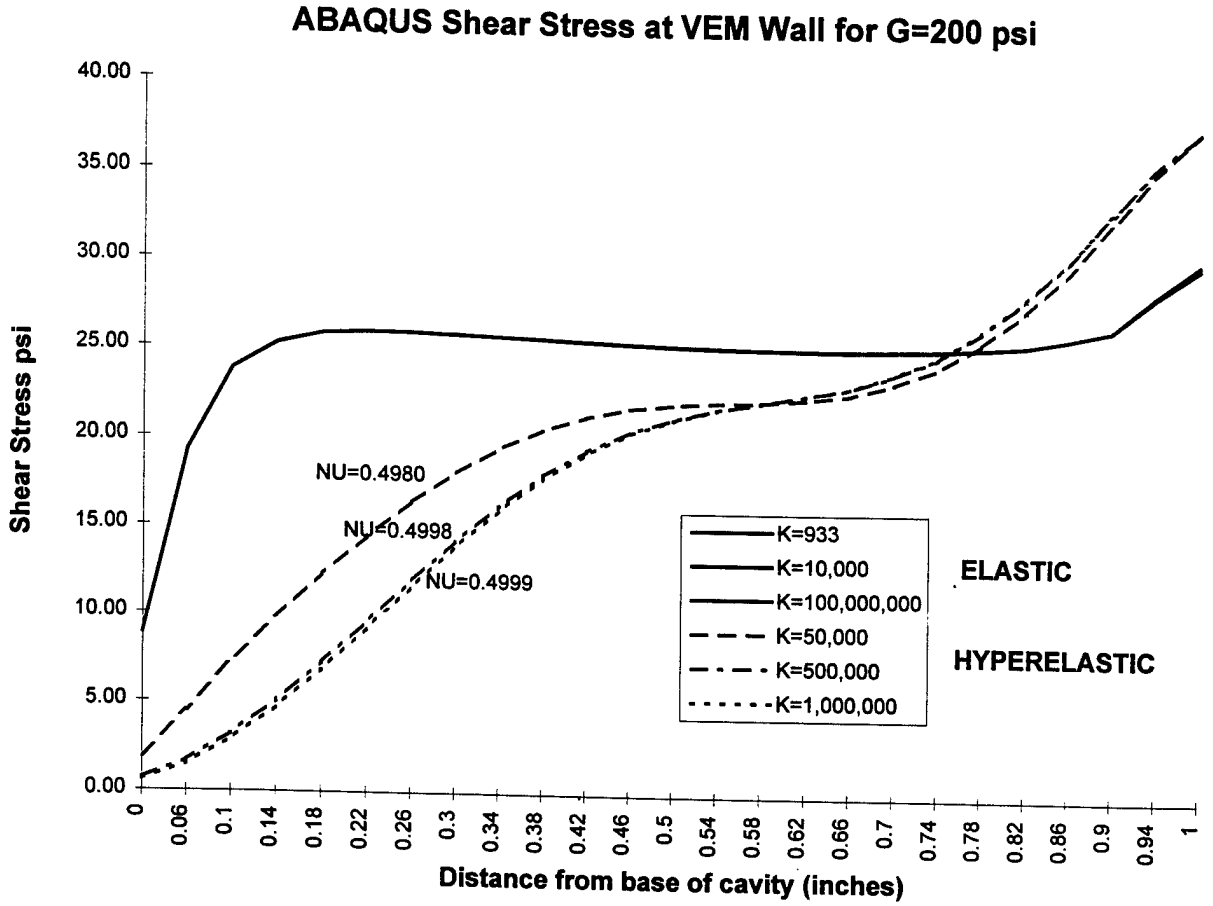

Figure 6. Plot illustrating the shear stresses in the VEM at the wall from hyperelastic analyses .

To check the limiting case, Poisson's ratio, υ, was allowed to go to 0.5, requiring a K of infinity. In this case, the hyperelastic model actually becomes the classical Mooney-Rivlin form. The maximum hydrostatic pressure increased to 261 psi from the 256 psi predicted for a K of one million, an amount of about two percent. The highest NASTRAN linear analysis predicted a stress of 251 psi, a difference of about four percent from the incompressible state. These results seem to show that the NASTRAN results, although not perfect, have a good degree of credibility.

In summary, variations in Poisson's ratio had only a minute effect on the hydrostatic pressures calculated by ABAQUS for the linear analysis, whereas both the NASTRAN linear analysis and the ABAQUS hyperelastic analysis predict higher and higher pressures at the base of cavity as υ approaches 0.5 (i.e. a state of incompressibility). For all cases, the pressure drops rapidly and becomes negative in the upper part of the cavity, putting the VEM into tension rather than compression. A second difference in the results is that the ABAQUS hyperelastic analysis predicts tension the rest of the way to the top surface, whereas NASTRAN results show the pressure returning to zero at the free surface. This comparison of the results of the ABAQUS hyperelastic analysis to the NASTRAN results appears to justify a conclusion that a nonlinear analysis is not necessary in this case. However, if creep and temperature dependent effects are introduced into the problem, a nonlinear approach may become necessary.

At this point, the reason as to why the ABAQUS linear analysis did not give identical results to NASTRAN is unknown. Resources available for this task did not allow this effect to be studied further. It is possible that boundary conditions applied to the ABAQUS model did not correspond exactly to the NASTRAN boundary conditions since they were partly translated by PATRAN and partly created by hand. However, a careful review of both models failed to find any errors. A review of displacements also indicated all displacements were approximately equal, leading to a belief that the problem lies with the ABAQUS program.

In retrospect, a specific finite element model made specifically for this analysis should have been constructed. A complete one-quarter blade model could have been constructed with simpler boundary conditions that would not have distracted attention from the results, particularly at the top surface of the VEM cavity.

In order to evaluate the validity of the FE part of this study, some simple theoretical studies were made in order to establish limits for the pressures and shears to be expected. These results are given in the following section.

5.0 THEORETICAL ANALYSES

We can put an upper limit on the hydrostatic pressure that can be generated by considering a rotating blade containing a thin cavity with rigid frictionless walls filled with an incompressible viscoelastic material. Starting from the basic equation, **F = ma** , the centrifugal force on a small cross-sectional area at radius r in the cavity as shown in figure 7 is:

$$\Delta F = (\rho A \Delta r)(r\omega^2) \qquad (1)$$

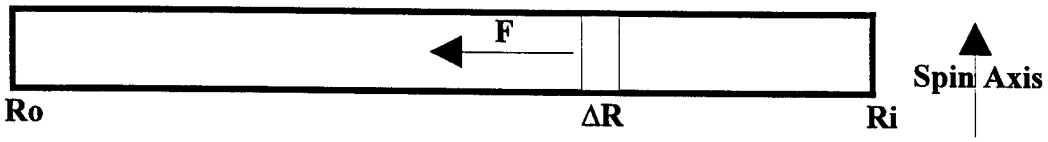

Figure 7. Plot illustrating centrifugal force in a frictionless cavity .

Integrating this equation from the inner radius R_i to any point r yields the following equation for the accumulated centrifugal force at r for a column of VEM:

$$F(r)/A = \sigma(r) = \rho\omega^2(r^2 - R_i^2)/2 \qquad (2)$$

Using parameters from the previous sections:

ρ = .0001117 lb-mass

ω = 7,500 rpm = 735.4 rad/sec

R_i = 13.875 inches

R_o = 14.875 inches

We obtain $\sigma(R_o)$ = 866 psi as the pressure exerted by the VEM column on the base of the cavity. This is also the pressure exerted on the side walls at this point, and can be shown to decrease toward the cavity surface as a function of $(1-R_i^2/r^2)$. This maximum pressure is more than three times as high as the finite element analysis results in the previous section, illustrating the relief afforded by the shear on the cavity walls.

The actual finite element model had walls that were stiff, but could deflect or bulge outward under an internal pressure. For theoretical purposes, if we assume flexible walls allowing a deformation that would double the cavity thickness, an incompressible VEM would be forced outward to occupy only the lower half of the cavity. Calculation shows that this only increases the maximum pressure by two percent to 883 psi for the finite element model used in this study. This small change can be attributed to this design having the VEM concentrated in a short cavity near the blade tip. A different design had been studied which had a 6.5 inch long internal pocket starting at a blade radius of 6.5 inches and extending to 13.0 inches. Using the rigid wall incompressible assumption and a same parameters, the maximum hydrostatic pressure at the cavity base comes out to be 3,828 psi because of the much longer VEM column. If the same flexible wall assumption is made, the pressure increases to 4,466 psi, an increase of seventeen percent.

An equivalent assumption to a flexible wall is to assume a compressible material. It can be shown that the change in volume under a uniaxial tension σ can be expressed as:

$$\Delta V/V = \varepsilon(1-2\nu) = \sigma(1-2\nu)/E.$$

Replacing σ by $\mathbf{F(r)/A}$ and $\mathbf{E}$ by $\mathbf{2(1+\nu)G}$, this becomes:

$$\Delta L/L = (F(r)/A)(1-2\nu)/2(1+\nu)G \qquad (3)$$

for our cavity. For a completely compressible material ($\nu = 0$) using the previous parameters, we get a $\Delta L/L$ of 2.165 at the base of the cavity. For a one inch column, this is an extension of 2.165 inches which gives a total column length of 3.165 inches. For compression, the volume or length change is the reciprocal of this factor, resulting in a column length of 0.31596 inches or less than a third of its original length. However, one must remember that this is true only for a cross-section at the base of the cavity where the centrifugal force is at its maximum, and that the compression decreases to zero at the top of the cavity.

It may be more instructive to look at the 6.5 inch pocket model. For the same rpm, the compressed length would be less than a tenth of an inch per inch at the base radius of 13.0 inches. Taking the reciprocal, we could call this a compression factor of over a thousand percent. At the middle of the VEM column (9.75 inches), the compression reduces considerably to about 0.47 inches per inch for a compression factor of about two hundred percent.

Obviously, the compression of the VEM depends upon the Poisson's ratio. The following graph shows how the compression factor varies with ν for both cavity designs.

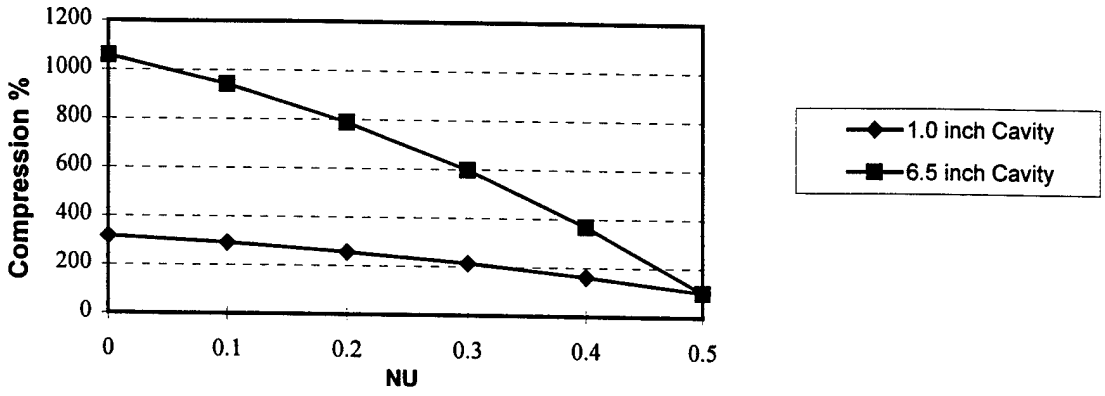

Figure 8. Plot illustrating compression of VEM in a frictionless cavity .

This plot shows that unless the VEM is nearly incompressible, typical centrifugal force can create a compression of several hundred percent, even in a cavity with rigid walls. When combined with flexible wall conditions, this effect could easily double, possibly resulting in extremely high hydrostatic pressures at the base. The obvious conclusion is that the shear stress at the walls needs to be sufficient to prevent any significant movement of the VEM in the cavity.

We can calculate the shear stress necessary to resist the centrifugal force at any cross-section of unit width and a cavity thickness **t**, bounded by $\mathbf{R_1}$ and $\mathbf{R_2}$, as shown in figure 9, by applying equation 1.

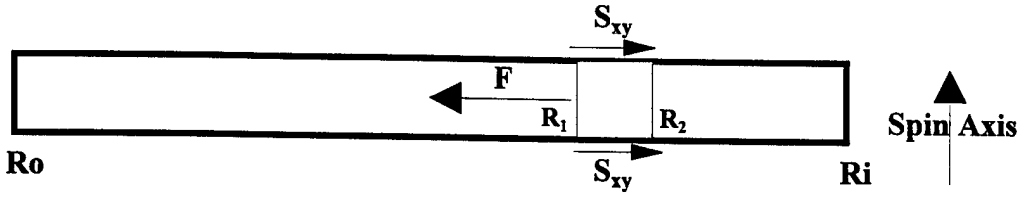

Figure 9. Plot illustrating the shear force in a VEM cavity .

This gives the centrifugal force at any local radius r as:

$$F(r) = t\rho\omega^2(R_1^2 - R_2^2)/2 \qquad (4)$$

The shear force S_{xy} on this cross-section equals **F(r)/2**. If we further bound the unit width cross-section so that the distance between R1 and R2 is a unit length, then S_{xy} becomes equal to $\tau_{r\theta}$. From equation (2), we see that $\sigma(r)$ equals **F(r)/t**, leading to the very simple relation:

$$\tau_{r\theta} = \sigma(r)t/2 \qquad (5)$$

Equation (5) describes the minimum shear stress that needs to be maintained on the cavity wall to keep the VEM from displacing toward the cavity base (i.e.; attached to the wall everywhere). Applying this equation to the one inch cavity where a hydrostatic pressure of 866 psi was predicted for the 0.06 inch thick cavity, we get 25.9 psi as the necessary wall shear stress. This correlates very well with the finite element analyses, especially the ABAQUS shear stresses predicted in figures 4 and 6 for any Poisson's ratio and to the NASTRAN results for a relatively compressible material.

If we do the same calculations for the 6.5 inch cavity, applying equation (4) to a one inch section at the base of the cavity (a radius of 13.0 inches) gives a pressure of 755 psi and a corresponding shear stress of 22.6 psi. This is a great improvement over the maximum hydrostatic pressure at the base of 3,828 psi predicted for a frictionless wall cavity. Making the same calculation at the center radius of the blade cavity (9.75 inches), we get a pressure of 589 psi and a shear stress of 17.7 psi. At the top of the cavity (6.5 inches), the pressure is 423 psi with a shear stress of 12.7 psi. The rate of decrease in shear along the walls as a function of the cavity radius is seen to be constant at about 1.5 psi per inch. The one inch long cavity is too short to illustrate this behavior clearly in the finite element analysis, although a small negative slope can be discerned in the upper part of the cavity in figure 4.

For the above shear calculations, no assumptions were made about compressibility or rigid wall conditions. These equations should apply even for a compressible material and flexible walls. If we assume both incompressibility and rigid wall conditions, we can conclude as stated earlier that $\sigma(r)$ will be a maximum of 3,828 psi at the base of the cavity and will decrease toward the cavity surface as a function of $(1-R_i^2/r^2)$. Due to incompressibility, the shear stresses for a rigid wall cavity will be identically zero and the total weight of the VEM column will be exerted on the case of the cavity. This is shown as case 1 in figures 10. Case 2 is a plot of the hydrostatic pressure based on the minimum shear stress necessary to hold the viscoelastic material in place. Cases 1 and 2 should represent limiting cases for the hydrostatic pressure plots in figures 3 and 5. The difference between the curves for cases 1 and 2 and the actual plots in sections 2 and 3 can therefore

be attributed to the flexible wall conditions. If we did allow flexible wall conditions for case 1, we would get slightly higher hydrostatic pressures as was shown previously, but then some shear stresses would also build up so the overall curves would not be much different than case 1 in figures 10 and 11.

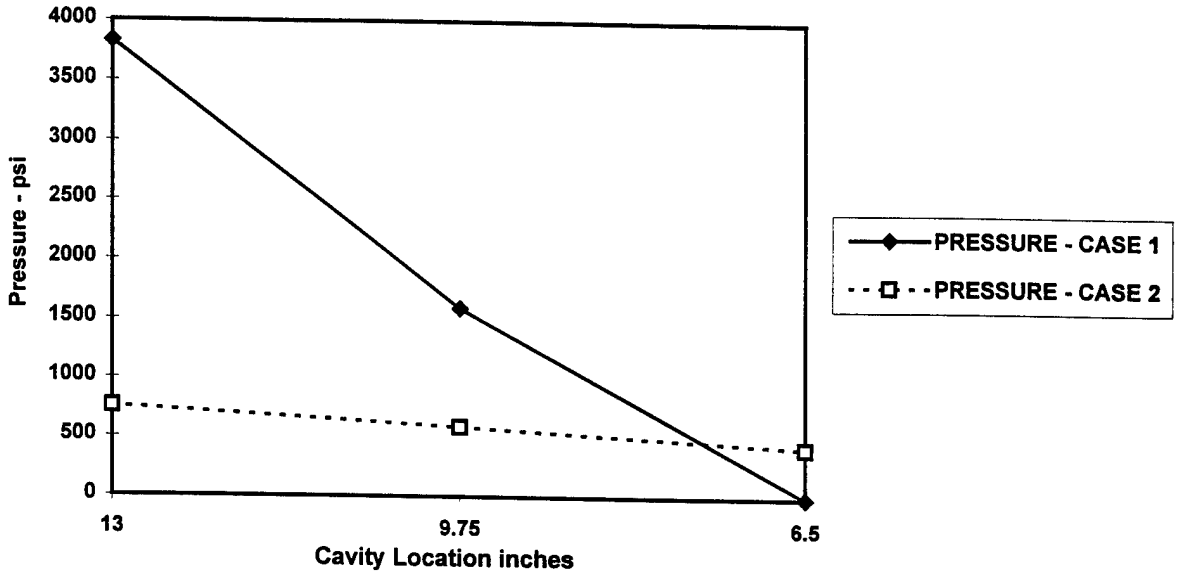

Figure 10. Plot illustrating theoretical hydrostatic pressure in a VEM cavity .

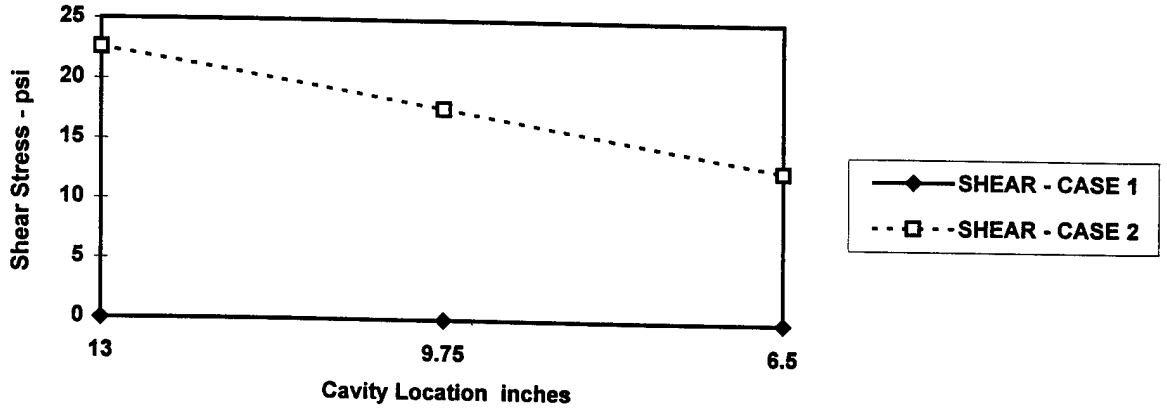

Figure 11. Plot illustrating theoretical shear stress in a VEM cavity .

It is concluded that for a 6.5 inch cavity blade model, finite element analysis would predict results that fall somewhere between these the two curves on the above two plots. Therefore the behavior of the predicted stresses from NASTRAN and the hyperelastic behavior predicted by ABAQUS appears to be realistic and credible.

6.0 CONCLUSIONS

The main conclusion reached in this report is that a finite element analysis performed with NASTRAN appears to provide results that are consistent with engineering logic and supported by some simple theoretical analyses.

Attention is also called to the role that shear on the cavity walls plays and to the effect of the cavity thickness. The hydrostatic pressure in the cavity is independent of the thickness as shown in equation (2) but is definitely reduced by the retarding effect of the shear acting on the cavity walls. The shear stress, on the other hand, is directly proportional to the cavity thickness as is shown in equation (5). It can thus be reduced or increased by designing a cavity to be thinner or thicker as needed.